Wind Turbine Ice Detection Using AEP Loss Method - A Case Study

Jia Yi Jin[1], Timo Karlsson[2], Muhammad S. Virk[1]

[1]Arctic Technology & Icing Research Group, Faculty of Engineering Science & Technology, UiT – The Arctic University of Norway, 8505 Narvik, Norway.

5 [2]VTT Technical Research Centre of Finland, Espoo, Finland.

Correspondence to: Jia Yi Jin (jin.jiayi@uit.no)

Abstract. Ice detection of wind turbine and estimating the resultant production losses is challenging, but very important, as wind energy project decisions in cold regions are based on these estimated results. This paper describes the comparison of a statistical (T19IceLossMethod) and numerical (Computational Fluid Dynamics, CFD) case study of wind resource assessment

10 and estimation of resultant Annual Energy Production (AEP) due to ice of a wind park in ice prone cold region. Three years Supervisory Control and Data Acquisition (SCADA) data from a wind park located in arctic region is used for this study. Statistical analysis shows that the relative power loss due to icing related stops is the main issue for this wind park. To better understand the wind flow physics and estimation of the wind turbine wake losses, Larsen wake model is used for the CFD simulations, where results show that it is important to use the wake loss model for CFD simulations of wind resource

15 assessment and AEP estimation of a wind park. A preliminary case study about wind park layout optimization has also been carried out which shows that AEP can be improved by optimizing the wind park layout and CFD simulations can be a good tool.

1 Introduction

Due to increasing demand of electrical power and needs of protecting the environment, there has been a growing need of rapid

20 expansion and better use of renewable energy resources to reduce the carbon emissions. Cold regions have good wind resources, but environmental challenges such as icing has been recognized as hindrance in proper utilization of these good wind resources. Worldwide, installed wind energy capacity in ice prone cold regions in 2015 was 86.5 GW, which is expected to reach 123 GW in year 2020. (Davis N., 2014) Therefore, wind resource assessment in cold regions is important both for the operation of wind parks and also to provide more accurate wind energy production forecasts. (IEA Wind Task 19, 2018) The

25 assessment of wind resources at cold climate sites is challenging and include aspects as terrain topology of the area where the wind park is to be located, wind behaviour, type of buildings or any other human intervention around the wind park location that may induce changes in the terrain roughness as well as the geometry of the wind turbine and its expected performance in the calculation of the tested scenarios. Low temperatures and icing climate set additional challenges for wind resource assessment in cold regions.

30 The International Energy Agency (IEA) T19 set out a statistical method to assess production losses due to icing based on standard SCADA data available from modern wind parks, named 'T19IceLossMethod' and developed by international expert group IEA Wind TCP Task 19. (IEA Wind Task 19, 2018) T19IceLossMethod is the standardized open source Python code model (IEA Wind Task 19, 2019) for assessment of wind power production loss (IEA Wind Task 19, 2018) and compared different sites with a systematic analysis method, as well as evaluate the effectiveness of various blade heating systems.

35 (Lehtomäki et al., 2019) The scope of work includes a detailed historical SCADA data analysis using 10-minute averages from four different wind turbine models and analysis of icing conditions on sites. (T19IceLossMethod, 2019)

CFD based wind resource assessment can provides improved agreement with the field measurements, when compared with the statistical flow models. Gravdahl et al. (Davis et al., 2016) performed CFD analysis for wind resource assessment and wind park design layout optimization, where they found that design of a wind park layout based upon CFD simulations can help to

40 increase the wind energy production. Wind turbine wake effects are important for the wind resource assessment and can be responsible for approximately 10- 20% losses of the AEP. (Bilal, 2016) Wind turbine wake effects on neighboring turbines effects the flow behavior, which also effects the wind turbine performance and power production. The development of models to describe wind turbine wake effects on energy production, include different initiatives of simplified or linearized models such as Jensen model (Katic et al., 1986) or more complex such as the eddy viscosity together with Gaussian shape, (Anderson,

45 2009; Renke, 2007) or second order model combined with the Prandtl's assumption of velocity been function of the distance power -1/3, (Larsen, 1988) or considering turbulence on the wake recovery as function of the distance from the wind turbine. (Ishihara et al., 2004) Wake structure creates a flow disturbance behind the wind turbine as well as in front of the turbine, which differ from the flow around an idealized turbine, (Longatt and Terzija, 2012) as shown in Figure 1.
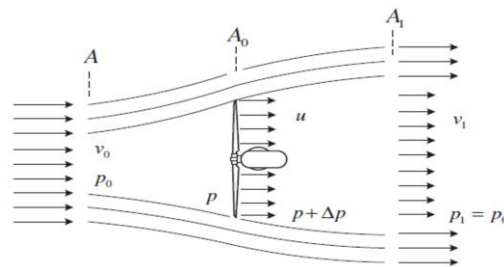
50 **Figure 1: Air flow near idealized wind turbine rotor.** (Longatt and Terzija, 2012)

Wake losses and aerodynamic behavior of wind turbine can be better addressed once the flow over the wind park site is better understood. Wind flow over steep slopes and ridges causes flow separation which is hard to capture and simulate using mesoscale models such as WRF. Furthermore, the atmospheric stability influences the wind flow. (Bilal et al., 2015) This paper describes the statistical and numerical case study of wind resource assessment and wind park design layout effects on

55 energy production in icing climate. T19IcelossMthod based statistical analysis and CFD based numerical simulations are carried out in comparison with the three years (2013-2015) wind park SCADA data. To better understand the wind turbine wake effects on flow behavior and resultant power production, Larsen wake model is used to calculate the AEP of each wind turbine.

2 Wind Park Terrain & Layout

60   Wind park used for this study consists of 14 wind turbines located at 400 m a.s.l in the arctic region of Norway. Three years (2013-2015) Supervisory Control and Data Acquisition (SCADA) from all wind turbines is collected and sorted for this study. This data mainly includes wind speed, wind direction, temperature and power production. Wind park terrain is hilly and is mainly covered with grass in summer and snow in winter. Figure 2 shows the wind park layout, terrain and wind rose map.
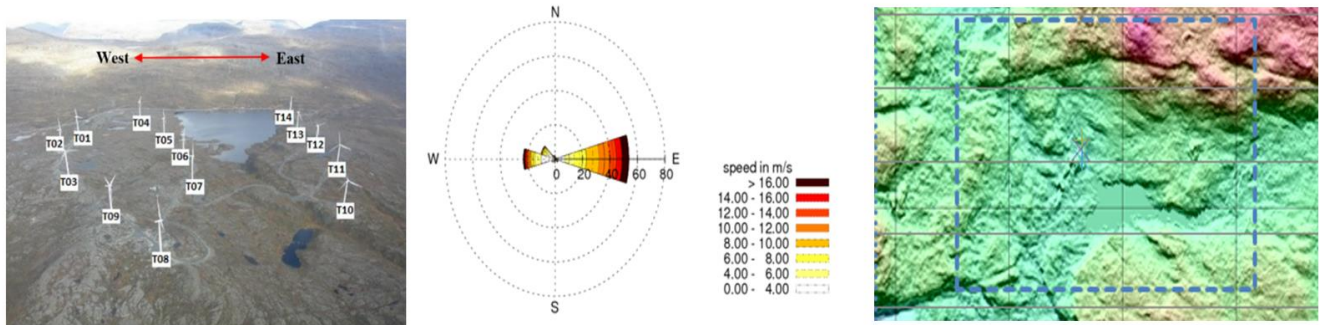
65   **Figure 2: Wind park layout & wind rose map.**

Wind direction is divided in 12 sectors, where first sector is oriented directly north. Wind climatology is presented as a wind rose, giving the average wind speed distribution divided in the velocity intervals (bins) and wind directions (sectors). The frequency distribution has been fitted to a Weibull distribution. Results of wind climatology for all 12 sectors are given in Table 1.

70   **Table 1: Average wind speed, frequency and Weibull shape (k) and scale (A) parameters.**

		Wind speed (m/s)			Frequency (%)			Weibull shape, k			Weibull scale, A		
Year		*2013*	*2014*	*2015*	*2013*	*2014*	*2015*	*2013*	*2014*	*2015*	*2013*	*2014*	*2015*
	01	1.62	2.63	6.30	1.14	1.84	33.08	0.92	1.23	2.16	1.70	2.84	7.46
	02	1.02	2.59	14.28	0.66	1.20	3.52	1.00	1.25	8.39	1.08	2.81	16.47
	03	8.51	1.44	2.30	24.32	0.92	1.39	2.79	1.15	0.64	10.12	1.64	1.37
	04	6.39	9.29	9.36	44.19	56.45	34.37	2.12	2.05	1.52	7.70	10.60	9.97
	05	1.94	7.29	6.19	0.98	12.08	4.72	1.06	1.57	1.56	2.02	8.45	6.90
Sector	**06**	1.83	2.36	4.40	0.88	0.45	0.27	1.17	1.24	0.90	1.91	2.52	3.60
	07	2.91	2.10	3.73	0.61	0.47	0.18	1.03	1.42	0.67	2.78	2.26	2.17
	08	3.62	3.78	4.07	1.38	1.10	3.17	1.43	1.51	1.44	4.09	4.31	4.56
	09	3.79	3.33	3.22	7.08	1.59	4.82	1.10	1.34	0.89	3.94	3.68	3.13
	10	4.36	4.60	5.48	16.08	11.63	10.40	1.62	0.89	1.18	5.16	3.99	5.48
	11	2.90	3.99	4.27	2.16	9.93	3.78	1.04	1.38	0.93	3.22	4.44	3.82
	12	1.96	3.95	3.39	0.52	2.35	0.29	1.06	2.03	1.33	1.80	4.72	3.69

3 Model Setup

3.1 Statistical Model

SCADA based T19IceLossMethod is the statistical model developed to minimize the required inputs and to create a solution that would not require any external measurements, such as ice detectors. Iced wind turbine power losses are defined by
75 comparing the performance to the calculated power curve using heated anemometers from nacelle and the measured reference, expected power curve. In general, the method can be divided into three main steps (IEA Wind Task 19, 2018) and site air density and air pressure are used to calibrate the nacelle wind speed as Eq. (1):

$$\omega_{site} = \omega_{std} \times \left(\frac{\rho_{std}}{\rho_{site}}\right)^{\frac{1}{3}} = \omega_{std} \times \left(\frac{\frac{\rho_{std}}{T_{std}}}{\frac{\rho_{site}}{T_{site}}}\right)^{\frac{1}{3}} = \omega_{std} \times \left(\frac{T_{std}}{T_{site}}(1 - 2.25577 \times 10^{-5} \times h)^{5.25588}\right)^{\frac{1}{3}} \qquad (1)$$

where ω_{site} is calibrated nacelle wind speed, ω_{std} measured nacelle wind speed, T_{site} is nacelle temperature and T_{std} is
80 standard temperature of 15°C, which resulting to air density of 1.225 kg/m³ at sea level $P_{std} = 101325$ Pa ambient air pressure, h is site elevation in meters above sea level. (Engineering Toolbox, 2003) In order to detect production loss, a baseline needs to be established. Icing event is defined as a period of time when the output power of wind turbine is below a set limit in cold temperature. These limits are calculated form a subset of the data where temperature is high enough so that it is reasonable to assume that there is very little icing. The detailed setup is described in Table 2.

85

Table 2: Setup of T19IceLossMethod.

Site elevation (m)	400.0
Wind speed bin size (m/s)	1.0
Reference temperature (ºC)	+1
Power curve lower limit	P10 (10% of power in the bin)
Power curve upper limit	P90 (90% of power in the bin)

The statistical model uses the 10th percentile of the power curve to trigger an icing alarm. The percentile method was chosen mainly due to robustness and simplicity of the definition (Engineering Toolbox, 2003) This method classifies icing events into three main categories: *Class a* means the reduced production due to icing, *Class b* means the stop caused by icing and *Class c*
90 is apparent over production. (T19IceLossMethod, 2019)

Most common icing effect on turbine operation is production loss, and the production losses are caused by degraded aerodynamics of the blade caused by ice accretion along the blade surface. If turbine stops during an icing event, it is assumed that the icing event is considered to be a contributing factor to the stop, where an icing induced stop is assumed to be ended once turbine output power is above the icing alarm limit again. In some cases turbine seems to be producing more than
95 expected, this can happen if for example an anemometer is experiencing icing. An iced cup anemometer will show lower wind speeds than what the actual wind speeds are. This in turn will result in apparent overproduction in SCADA.

3.2 Numerical Model

CFD based numerical simulations are carried out using WindSIM software, which is a modern Wind Park Design Tool (WPDT) that helps to optimize the wind park energy production by using non-linear mathematical methods. 3D terrain model
100   of the wind park is generated where the domain is discretized using hexahedral numerical grid. Iterative numerical simulations of air flow behavior are performed by solving Reynolds Averaged Naiver-Stokes equations (RANS). The energy equation is neglected during this study, as temperature is assumed constant in the region close to the ground surface. So, the exchange of heat and water vapour at the Earth's surface is neglected. In order to account for surface roughness in the numerical simulations, Wieringa's classification is used. RNG-based k-ε turbulence model is used due to its better agreement with the flow profiles
105   and length of the separated flow region. The detailed setup is shown in Table 3.

Table 3: Solver setting for CFD simulations.

Height of boundary layer (m)	500.0
Speed above boundary layer (m/s)	10.0
Boundary condition at the top	fix pressure
Potential temperature	No
Turbulence model	RNG k-ε

The default value of terrain surface roughness heights is read from the grid file in WindSIM, or, alternatively a constant roughness height can also be imposed in the model by specifying a non-zero value for the roughness height. The roughness
110   height is used in the velocity profile log-law, given in Eq. (2):

$$\frac{u}{u^*} = \frac{1}{\kappa} \ln z/z_0 \qquad (2)$$

where u is the wind velocity; u* is the friction velocity, κ is von Kármán constant (κ = 0.435); z is the coordinate in vertical direction; z_0 is the roughness height. Wind park digital terrain layout used for the CFD simulations is shown in Figure 3.
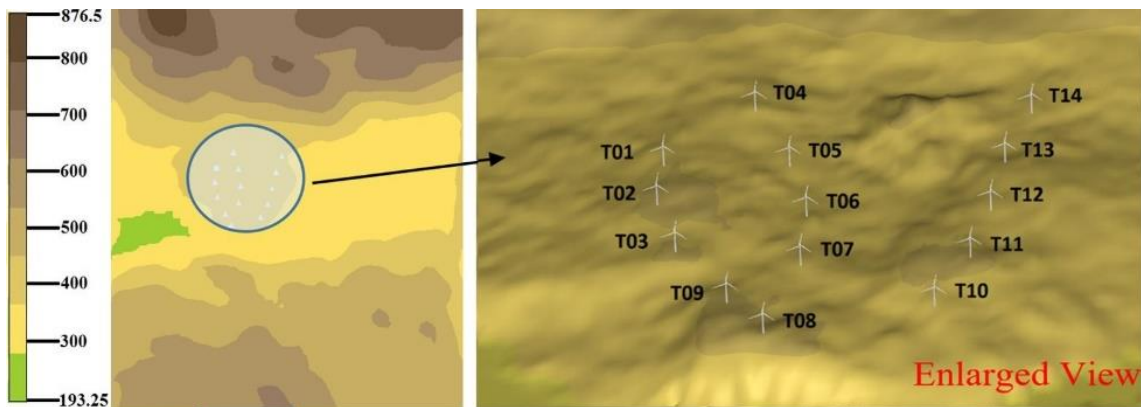
115
Figure 3: Digital terrain (m) of wind park layout.

In this study, the wind park terrain corresponds to mesoscale topology of the region around the wind park. The areas selected for the wind flow simulations is the section that involves different sizes in the direction of the flow to determine the influence

of the natural formation of the region on the wind profile. In the wind park terrain, the presence of a natural channel along the

mountain line west-east oriented at the north side and water body at the south represent a challenge for the selection of the

120   domain to do the numerical simulations. Estimation of latitudinal and longitudinal extension of the domain is quite important

because the wind behavior will be directly affected by the surface shape, following the mass and momentum conservation

equations. For a fixed latitude range that cover the top of the mountain and a more flatter area to the south, three different

territorial domains based on the variation of the starting point of the domain in the longitudinal direction are tested in this

numerical study. Mesh sensitivity analysis are carried out, where a final refined mesh by default placed in the centre of the

125   domain and the cell distribution is uniform within the refined area with an increasing cell size towards the borders with cell

resolution of 28m is selected for the numerical study. Figure 4 shows the numerical mesh used for this study, the grid spacing,

and cells is described in Table 4.
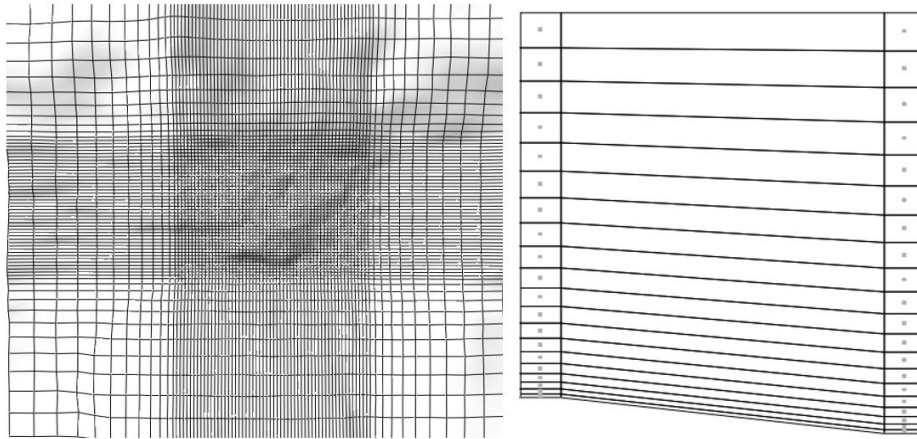
Figure 4: Horizontal layers (left) and vertical layers (right) of the 3D model, used for grid generation.

130   **Table 4: Gird Spacing and cells.**

	East	North	z	Total
Grid spacing (m)	61.8-454.8	61.0-439.0	Variable	-
Number of cells	78	64	20	99840

Larsen et al. wake loss model (Anderson, 2009) is used for this study. This wake loss model is based on calculating the

normalized velocity deficit and rotational axisymmetric along the x-axis, δV, as described in Eq. (3):

$$\delta V = \frac{U - V}{U} \tag{3}$$

135   where, U is the free stream velocity, and V is air velocity at some point after the turbine rotor. This model is derived from the

turbulent boundary layer equations and a similarity assumption. Shows as Eq. (4):

$$\delta V = \frac{1}{9}(C_T A_r x^{-2})^{\frac{1}{3}} \left\{ r^{\frac{3}{2}} (3C_1{}^2 C_T A_r x)^{-\frac{1}{2}} - \left(\frac{35}{2\pi}\right)^{\frac{3}{10}} (3C_1{}^2)^{-\frac{1}{5}} \right\}^2 \tag{4}$$

where, C_T is the thrust coefficient, and the constant A_r and variable C_1 based on rotor diameter (m) D, are described in Eq. (5) and (6):

$$A_r = \frac{\pi D^2}{4} \tag{5}$$

$$C_1 = \left(\frac{D}{2}\right)^{\frac{5}{2}} (C_T A_r x_0)^{-\frac{5}{6}} \tag{6}$$

where, x_0 is described in Eq. (7), and referred to R_{95} which described by using R_{nb} that correlated with the ambient turbulence intensity at hub height, I_a, as shown in Eq. (8) and (9):

$$x_0 = \frac{9.5D}{\left(\frac{2R_{95}}{D}\right)^3} - 1 \tag{7}$$

$$R_{95} = 0.5\big(R_{nb} + min(h, R_{nb})\big) \tag{8}$$

$$R_{nb} = max(1.08D, 1.08D + 21.7D(I_a - 0.05)) \tag{9}$$

4 Results and Discussion

4.1 Ice Detection

Result from T19IceLossMethod are compared with the field SCADA data from the wind park. All three categories of icing events: *Class a, Class b and Class c* are used as relative production losses due to icing (% of kWh), relative losses due to icing related stops (% of kWh) and over production hours (% of total hours) respectively. The results from this statistical model are shown in Table 5, and the calculation of losses time of all icing events is illustrated in Table 6. The maximum values are shown with pink color and the minimum values are shown with green color.

155

Table 5: Classification of icing events detected by T19IceLossMethod.

	Class a			Class b			Class c		
Year	*2013*	*2014*	*2015*	*013*	*2014*	*2015*	*2013*	*2014*	*2015*
01	**2.1**	**0.3**	0.2	8.9	1.3	**13.4**	*0.4*	3.0	2.6
02	0.5	**0.3**	0.2	**9.1**	3.4	8.8	0.7	3.0	*1.0*
03	0.3	0.2	0.3	5.3	1.6	4.9	1.7	3.8	1.6
04	0.2	0.2	*0.1*	2.3	1.3	2.1	**3.0**	3.7	**4.2**
05	0.2	0.2	*0.1*	2.6	*0.8*	1.6	2.6	3.1	2.6
06	0.2	0.2	0.2	2.1	1.5	1.6	1.6	3.1	2.4
07	0.2	0.2	0.4	*2.0*	1.3	*1.2*	1.0	3.8	2.2
08	0.2	0.2	**0.5**	2.4	3.5	2.8	1.0	3.6	2.0
09	0.2	0.2	0.3	3.4	2.8	2.9	2.6	**4.2**	2.2
10	0.2	*0.1*	*0.1*	4.3	1.5	2.0	1.3	4.0	1.8
11	*0.1*	0.2	0.2	5.2	1.8	1.9	1.1	*2.1*	1.2
12	*0.1*	*0.1*	0.2	3.0	1.1	3.9	2.4	3.6	1.6
13	*0.1*	0.2	*0.1*	4.4	**29.6**	4.1	0.5	3.1	2.8
14	*0.1*	0.2	*0.1*	2.1	3.1	4.3	1.6	3.1	1.6

Table 6: Classification of losses time (hour) of icing events detected by T19IceLossMethod.

	Class a of time			Class b of time			Class c			% loss of total hour		
Year	*2013*	*2014*	*2015*	*2013*	*2014*	*2015*	*2013*	*2014*	*2015*	*2013*	*2014*	*2015*
01	**6.6**	**2.3**	*0.4*	12.2	*6.6*	3.0	*0.4*	**12.2**	2.6	**19.2**	*11.9*	**15.5**
02	1.4	2.1	0.7	11.5	8.7	3.0	0.7	9.5	*1.0*	13.6	13.8	12.0
03	1.3	1.5	1.7	10.8	6.8	3.8	1.7	6.6	1.6	13.8	12.1	*9.5*
04	1.0	1.6	**3.0**	10.7	7.5	3.7	**3.0**	6.6	**4.2**	14.7	12.8	11.5
05	0.6	*1.0*	2.6	11.4	8.5	3.1	2.6	7.0	2.6	14.6	12.6	10.1
06	0.7	*1.0*	1.6	11.5	10.1	3.1	1.6	7.3	2.4	13.8	14.2	10.4
07	1.0	1.1	1.0	12.0	9.2	3.8	1.0	7.3	2.2	14.0	14.1	10.4
08	1.0	1.6	1.0	11.4	10.2	3.6	1.0	7.0	2.0	13.4	15.4	10.4
09	0.8	1.5	2.6	11.4	8.4	**4.2**	2.6	*6.4*	2.2	14.8	14.1	9.8
10	0.8	*1.0*	1.3	11.4	9.5	4.0	1.3	7.8	1.8	13.5	14.5	10.4
11	0.8	1.1	1.1	**13.6**	9.1	*2.1*	1.1	7.4	1.2	15.5	12.3	9.6
12	0.7	1.2	2.4	11.8	8.9	3.6	2.4	7.9	1.6	14.9	13.7	10.4
13	*0.4*	1.1	0.5	11.5	**19.6**	3.1	0.5	7.4	2.8	12.4	**23.8**	11.0
14	0.6	1.5	1.6	*9.8*	8.3	3.1	1.6	9.7	1.6	*12.0*	12.9	11.6

According to the statistical method, the bold and underlined data zones are where the maximum power losses in each icing

160   event categories, which means annual power production is not ideal in these turbines, and need to optimize the wind turbine

sites or operation methods to improve the actual wind power productions. Whereas the bold and italicized data zones are the

minimum power losses where the actual wind energy production is ideal in these turbines. To consider the operating hours of

each turbines during year 2013 to 2015, turbine 01 are the maximum loss of total hours in 2013 and 2015. However, turbine

01 in 2014 has the minimum and turbine 13 has the maximum loss of total operating hours. Results of maximum ice loss
165 detection on wind power production for turbine 01 and turbine 13 are shown in Figure 5 by using 10th (P10) and 90th (P90)
percentile of power in the bin compared with standard power production with median output power in the bin.
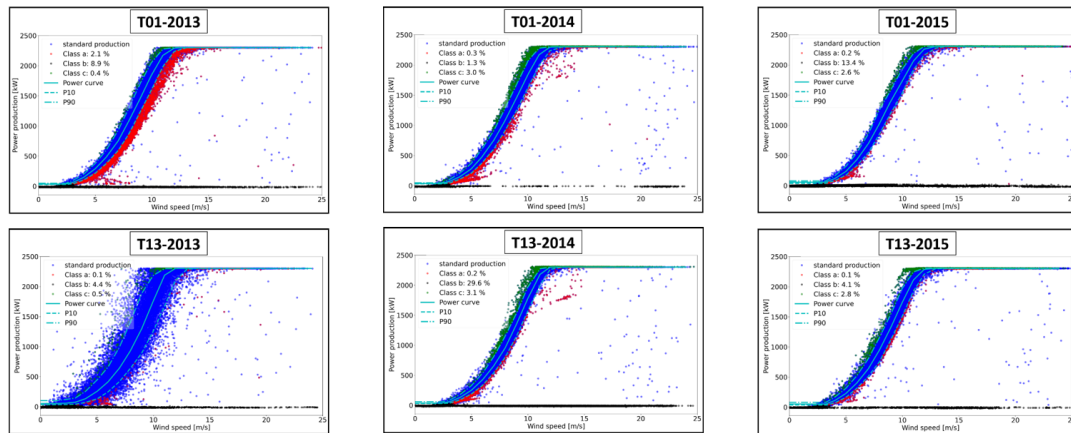
Figure 5: Ice detection of T01 and T13 during 2013 to 2015.

Analysis shows that the maximum reduced power production due to icing with T01 is 2.1% in 2013, 0.3% in 2014 and T08 is
170 0.5% in 2015, whereas the maximum ice loss with *class a* for all 14 wind turbines. Analysis about the maximum stop caused
by icing with T02 is 9.1% in 2013, T13 is 29.6% in 2014 and T01 is 13.4% in 2015 respectively, where the maximum ice loss
with *class b* for all 14 wind turbines. For the ice loss with *class c* for all 14 turbines, analysis shows that T04 is 3.0% in 2013,
T09 is 4.2% in 2014 and T04 is 4.2% in 2015 with the maximum apparent overproduction. In total, added up ice losses in
different categories of all 14 wind turbines, *class b* is the maximum ice detection category for all three years of the wind park,
175 with 57.1%, 54.6% and 55.5% respectively, whereas *class a* is the minimum ice detection category during 2013 to 2015 with
ice loss 4.7%, 2.8% and 3.0% separately. In other words, the relative power losses due to icing related stops are the main issue
for this wind park.

4.2 Wind Resource Assessment

Results from CFD simulations are compared with the field SCADA data from the wind park. Both simulated and measured
180 results of average wind conditions are used for AEP estimation. For the CFD simulations, three hub heights (35, 80 & 125 m)
which equal the lower and upper tip height and the hub height are used for the comparison. Wind resource maps for all three
hub heights are shown in Figure 6, where simulation results show that the wind park locates and operates in rich wind resources
area. The results from wind resource map also shows that wind speed at the hub height of 125m is the highest and 35m is the
lowest in all three years. The main reason for it is the planetary boundary layer effects, i.e. the friction near the surface, due to
185 no-slip condition, which results in some mass flux of the air being displaced into layers at higher altitudes, which by mass-
conservation principle will result in adjacent layers slowing down. In addition, according to the pioneer research work (Liu et
al., 2010) and the topographic characteristics of actual wind park with specific surface roughness height study in this paper,

when the airflow through the mountain and lake, the flow will form a recirculation zone. If the wind speed is high or the atmosphere structure is unstable, a strong vortex motion will appear on the leeward side of the mountain. This vortex motion

190   may cause the wind speed to rotate at a certain height, thus showing the phenomenon that wind speed decreases with height. This affects the velocity deficit in near-surface layers that result in change of wake and associated power losses.
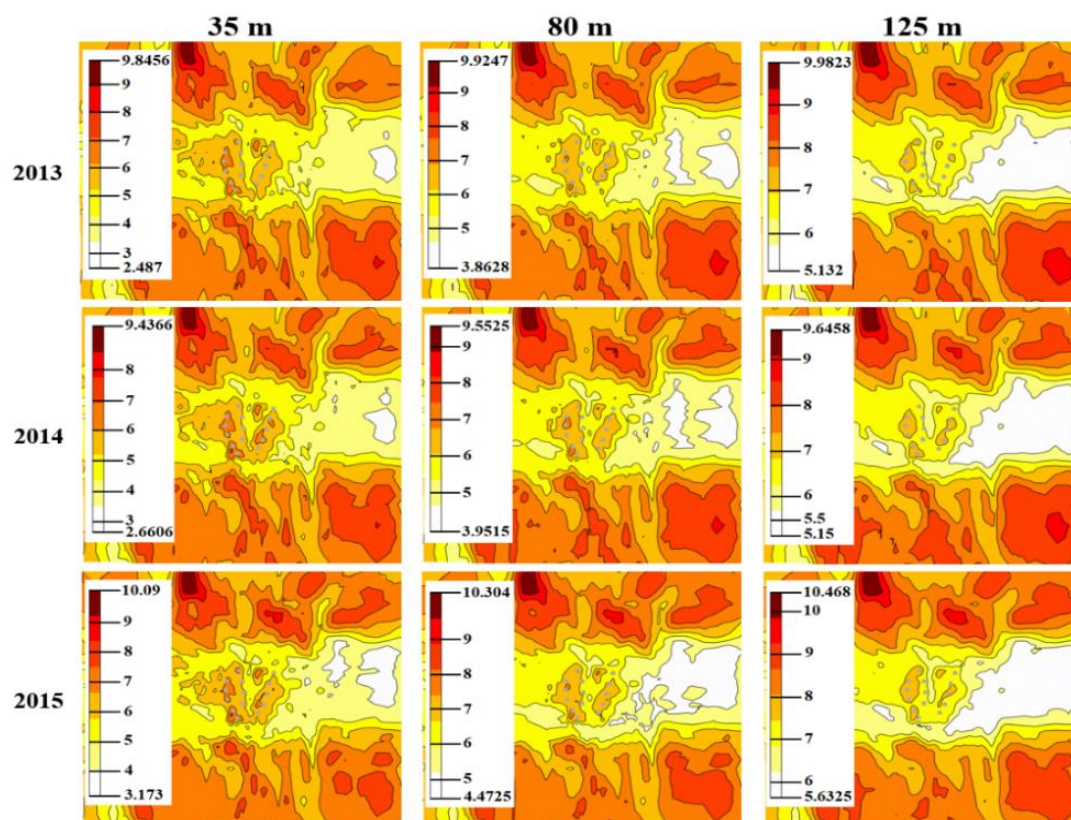
Figure 6: Wind resource map at hub height of 35, 80 & 125 m.

4.3 AEP Estimation and Comparison

195   Numerical analysis are carried out based on the geographical long-term conditions in order to calculate the AEP of the wind park using Larsen wake loss model with actual surface roughness height. Each year SCADA data is further analyzed and compared by T19IceLossMethod statistical model and CFD simulation. This approach is used to get the better estimate of energy based availability within field SCADA data, statistical model and numerical simulations of the wind park. In 2013 and 2015, both statistical and CFD results showed overestimated AEP values when compared with the SCADA data, whereas the

200   underestimated AEP values show mostly in 2014 for CFD simulations. In other words, the wind park have better estimation of energy power production compare in year 2013 and 2015. Then further CFD analysis are carried out by taking into account the wind turbine wake losses. Results of this parametric study are shown in Table 7 and Figure 7.

Table 7: Energy based availability (%) of SCADA with statistical and numerical model.

%	SCADA/T19IceLossMethod			SCADA/gross-CFD			SCADA/wake loss-CFD		
Year	*2013*	*2014*	*2015*	*2013*	*2014*	*2015*	*2013*	*2014*	*2015*
01	87.90	96.98	60.23	79.71	**101.50**	50.51	83.55	**105.90**	52.01
02	89.49	94.03	89.77	72.43	**101.21**	77.95	75.50	**104.86**	80.62
03	85.84	95.44	91.81	80.44	**109.20**	80.79	83.72	**113.26**	83.57
04	97.18	97.87	97.93	93.92	**104.18**	85.58	95.56	**105.99**	86.84
05	97.12	98.50	**101.61**	90.76	**118.54**	85.10	94.61	**123.04**	87.88
06	96.77	97.63	98.63	91.22	**111.06**	82.17	95.93	**116.07**	85.45
07	96.82	97.36	99.45	90.86	**101.07**	88.01	95.53	**105.48**	91.90
08	97.23	96.57	98.15	88.55	97.44	85.90	90.49	99.20	87.13
09	96.03	96.27	97.15	90.43	**105.40**	80.80	93.56	**108.40**	82.93
10	94.78	98.48	95.42	80.07	94.68	72.08	81.43	95.78	72.96
11	93.96	97.86	97.59	80.03	90.87	81.77	80.79	92.18	83.83
12	95.92	98.14	96.68	85.97	**101.75**	73.44	86.74	**102.76**	74.41
13	95.70	76.40	95.31	85.43	82.49	86.60	86.11	83.47	88.13
14	97.07	95.35	67.01	**101.86**	125.23	64.46	**102.53**	126.00	64.80
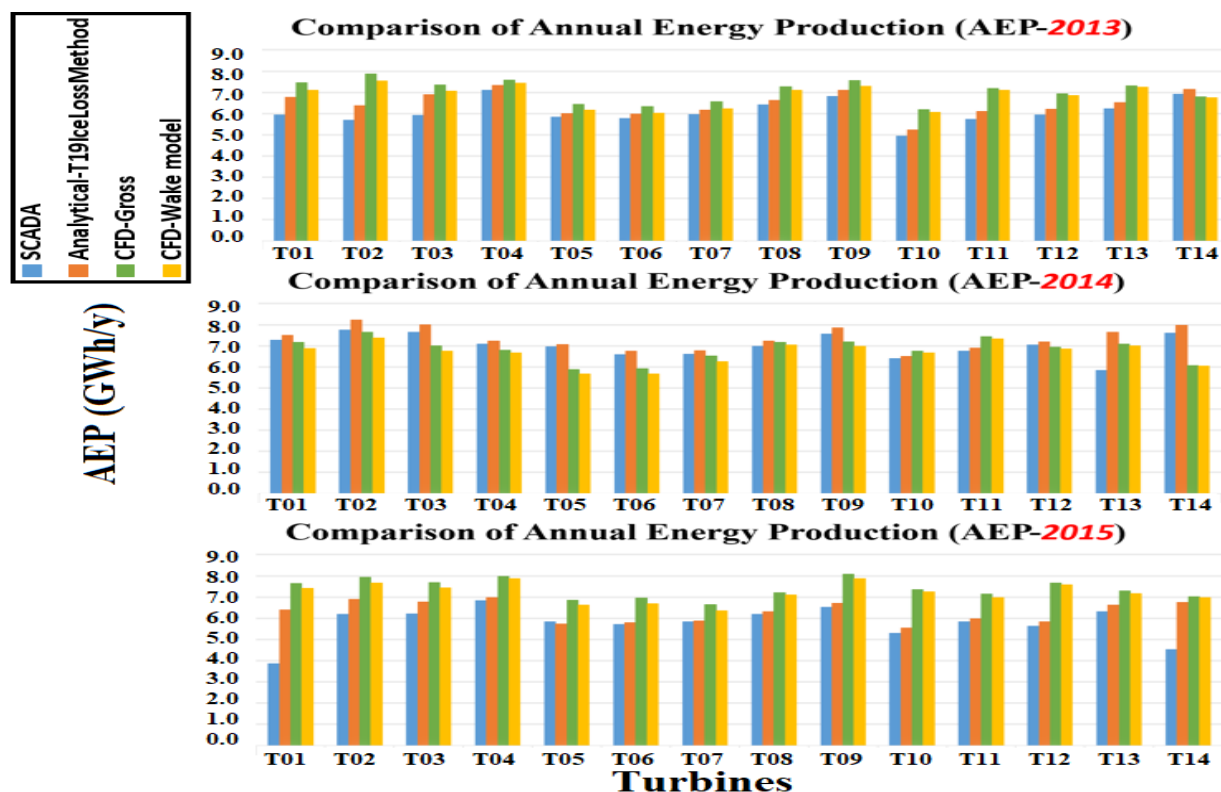
Figure 7: AEP comparison within SCADA, T19IceLossMethod and CFD simulation with or without wake effects for each wind turbine.

205

Analysis show that CFD results without use of wake model overestimated the AEP in comparison to SCADA data, whereas CFD results with the use of Larsen wake loss model is found in better agreement with the SCADA data in 2013 and 2015,
210 whereas for 2014 are in reverse. This case study highlights that it is important to use the proper wind turbine wake model for CFD analysis while performing the wind resource assessment.

4.4 Wind Park Layout Optimization

To further improve the AEP and reduce wake loss effects of the wind park, a preliminary numerical case study is carried out to optimize the existing wind park layout (wind turbine locations). WindSIM Park Optimizer is used for this purpose. Park
215 optimizer is a numerical tool coupled with the WindSIM that helps to maximize the wind farm profitability by optimizing the wind park layout. Park optimizer uses two type of optimization approaches, *1) basic optimization*, *2) WFD (wind farm design) optimization*. The basic optimization is based on heuristic algorithm which gives near optimal results. Algorithms such as genetic algorithm, simulated annealing and similar trial-and error algorithms for the wind park layout design also provide good results but they are slow in process and do not provide information about the quality. The WFD optimizer is highly innovation
220 approach based on formal research operation methods and is derived from state of art optimization solver. For this case study, we have used WFD optimizer. Results from CFD simulations of year 2014 presented in previous section are used as input to the WFD optimizer, where WFD optimizer optimally relocated the wind turbines with respect to the highest average wind speed and wind energy. Figure 8 shows the optimized layout of the wind park in comparison to existing layout.
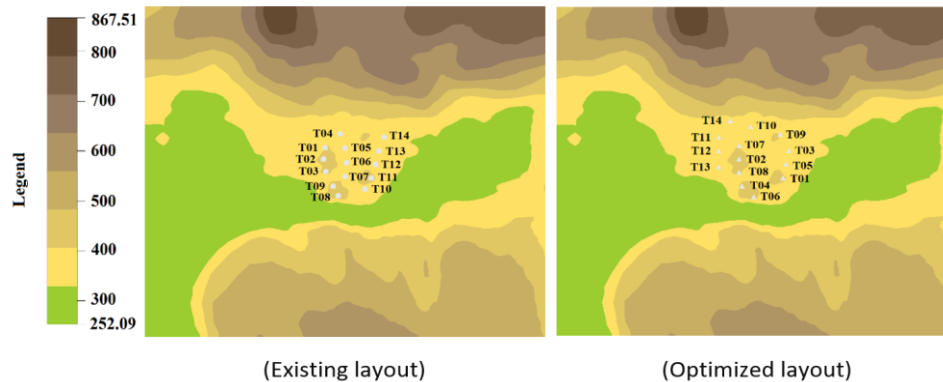
Figure 8: Existing wind turbines location and optimized wind turbines location.

Table 8: Comparison of gross AEP and total wake loss for optimized design layout of the wind park.

	Gross AEP (GWh/y)	Total wake loss (%)
SCADA	98.13	-
CFD – before optimization	95.61	35
CFD – after optimization	112	28

To verify that how much AEP is increased after optimization of the wind park layout, CFD simulations for optimized wind park layout are carried out. Larsen wake model is used for this study. Table 8 shows the AEP and total wake loss results of the

Wind Park. Before optimization of the wind park layout design, gross AEP from CFD analysis has been calculated as 95.61GWh/y, whereas after optimizing the wind park layout the gross AEP calculations from CFD simulations shows a value of 112 GWh/y. Comparison of AEP for optimized design layout of the wind park shows that 16.39 GWh/y energy increased as compared to the existing layout design. Moreover, the CFD based on Larsen wake model have decreased 7% in total wake loss compare before and after optimization used WFD optimizer. This shows that CFD based numerical optimization approach can be a good way to better simulate the wind resources and optimize the wind park layout and the power production.

5 Conclusion

SCADA data analysis, T19IceLossMehtod and CFD simulations are carried out for a wind park located in arctic region. AEP from SCADA data is compared with statistical and CFD simulations, where a good agreement is found. Statistical analysis shows the relative power loss due to icing related stops (Class b) is the main issue for this wind park from 2013 to 2015. While the CFD analysis shows that it is important to use the proper wake loss model for better estimation of the wind resources using numerical simulations. Analysis also show that CFD results without use of wake loss model can over/under-estimate the AEP in comparison to SCADA data, whereas CFD results with the use of wake loss models are in good agreement with the SCADA data. Analysis shows the phenomenon that wind speed decreases with height increase due to the wind park have a strong vortex motion appear on leeward side of the mountain and affects the velocity deficit in near-surface layers, which result in change of wake and associated power losses. Moreover, study about wind park layout optimization shows that AEP can be optimized by optimizing the wind park layout and CFD simulations can be used as a tool in this regards.

Code and data availability

T19IceLossMethod (T19IceLossMethod, 2019) is the standardized open source Python code model open-source simulation tools developed by international expert group IEA Wind TCP Task 19. The GitHub repository https://github.com/IEAWind-Task19/T19IceLossMethod. The SCADA data and other farm-specific information for the commercial wind farm discussed in Sect. 2 are not publicly available due to proprietary privacy restrictions.

Author contributions

JYJ conducted the main research work and prepared a first draft of the manuscript. TK developed the coding and software of statistical model, and assisted in the visualization and validation. MSV provided the guidance, methodology and resources, supervised the research. All authors provided important input to this research work through discussions and feedback and by improving the manuscript.

Competing interests

The authors declare that they have no conflict of interest.

Acknowledgments

260 The work reported in this paper is supported by the University of Tromsø PhD project no (381100/74104) and the publication charges for this article have been funded by a grant from the publication fund of UiT-The Arctic University of Norway. Authors would also like to thanks Dr. Matthew Carl Homola for technical support in this study.

References

Anderson, M., *Simplified solution to the Eddy-viscosity wake model, RES document 01327-202*. 2009.

265 Bilal M., Sridhar N., Araya G., Parameswaran S. and Birkelund Y., *Wind flow over complex terrain in Nygårdsfjell, Norway*, The American Sociry of Mechanical Engineers (ASME) proceeding: Energy Sustainability, San Diego, USA, https://doi.org/10.1115/ES2015-49188, October 27, 2015.

Bilal, M., *Wind Energy at Nygårdsfjellet-Norway: Wind field characterization and modelling*, Ph.D. thesis, Department of Physics and Technology, UiT-The Arctic University of Norway: Tromsø, 2016.

270 Bourgeois S., and Beckford T., *IEA Wind task 19 – wind energy in cold climates – available technologies report (2nd edition), 2018*.

Davis, N. N., Pinson P., Hahmann A.N., Clausen N.E. and Žagar M., *Identifying and characterizing the impact of turbine icing on wind farm power generation,* Wind Energy, 19,1503-1518, https://doi.org/10.1002/we.1933, 2016.

Davis N., *Icing Impacts on Wind Energy Production, Ph.D. thesis, The Department of Wind Energy*, DTU: Denmark, 2014.

275 Lehtomaki V., Krenn A., Jordaens P.J., Godreau C., Davis N., Yazami Z.K., Bredesen R.E., Ronsten G., Wickman H., IEA Wind Task 19, *T19IceLossMethod: Method for estimating icing losses from wind turbine SCADA data*, https://github.com/IEAWind-Task19/T19IceLossMethod. 2019.

Engineering ToolBox. *Altitude above Sea Level and Air Pressure*, https://www.engineeringtoolbox.com/air-altitude-pressure-d_462.html, 2003.

280 Ishihara, T., A. Yamaguchi, and Y. Fujino. *Development of a New Wake Model Based on a Wind Tunnel Experiment*, Glob.Wind Power, http://windeng.t.u-tokyo.ac.jp/ishihara/e/, 2004.

Katic I., Højstrup J., and Jensen N.O., *A Simple Model for Cluster Efficiency*, In W. Palz & E. Sesto (eds.), EWEC86 Proceedings, 1, 407-410. Rome, Italy, 7-9 October, 1986.

Larsen, G.C., *A Simple Wake Calculation Procedure*, Risø National Laboratory: Risø-M-2760, Roskilde, Denmark, 1988.

285 Liu M., Jie Sun J., Yang H.Q. and Yuan Y.C., *The Study on Wind Speed Change with Hight Under Different Terrain Conditions in Hubei Province*, Methorolygical Monthly, 36 (4): 63-67, 2010.

Longatt F.G. and Terzija P.W., *Wake Effect in Wind Farm Performance Steady-State and Dynamic Behaviour,* Renewable Energy, 39(1):329-338, https://doi.org/10.1016/j.renene. 2011.08.053, 2012.

Lehtomäki V., Karlsson T. and Rissanen S., *Wind Turbine Ice Protection System Benchmark Analysis*, VTT Technology 341,
290 VTT Technical Research Centre of Finland Ltd, 2018.

Renke, D.J., *Validation of wind turbine wake models. Using wind farm data and wind tunnel measurements*, Mater thesis, Department of Aerospace Engineering, Delft University of Technology: Netherland, 2007.

T19IceLossMethod, *Task 19 Ice Loss Release 2.2 tutorial*, https://github.com/IEAWind-Task19/T19IceLossMethod, 2019.